ISSN 1674-1056
http://cpb.iphy.ac.cn
http://iopscience.iop.org/cpb
中国物理 B
Chinese Physics
中国物理
Chinese Physics B

A method for calibrating the confocal volume of a confocal three-dimensional micro-x-ray fluorescence setup

Peng Zhou(周鹏), Xin-Ran Ma(马欣然), Shuang Zhang(张爽), Tian-Xi Sun(孙天希), Zhi-Guo Liu(刘志国)
Citation: Chin. Phys. B . 2020, 29(2): 020702 . **doi:** 10.1088/1674-1056/ab671c
Journal homepage: http://cpb.iphy.ac.cn; http://iopscience.iop.org/cpb

What follows is a list of articles you may be interested in

Detailed calibration of the PI-LCX: 1300 high performance single photon counting hard x-ray CCD camera

Wei Hong(洪伟), Xian-Lun Wen(温贤伦), Lai Wei(魏来), Bin Zhu(朱斌), Yu-Chi Wu(吴玉迟), Ke-Gong Dong(董克攻), Chun-Ye Jiao(焦春晔), Bo Wu(伍波), Ying-Ling He(何颖玲), Fa-Qiang Zhang(张发强), Wei-Min Zhou(周维民), Yu-Qiu Gu(谷渝秋)
Chin. Phys. B . 2017, 26(2): 025204 . **doi:** 10.1088/1674-1056/26/2/025204

An efficient calibration method for SQUID measurement system using three orthogonal Helmholtz coils

Hua Li(李华), Shu-Lin Zhang(张树林), Chao-Xiang Zhang(张朝祥), Xiang-Yan Kong(孔祥燕), Xiao-Ming Xie(谢晓明)
Chin. Phys. B . 2016, 25(6): 068501 . **doi:** 10.1088/1674-1056/25/6/068501

Fast synchrotron X-ray tomography study of the packing structures of rods with different aspect ratios

Zhang Xiao-Dan, Xia Cheng-Jie, Xiao Xiang-Hui, Wang Yu-Jie
Chin. Phys. B . 2014, 23(4): 044501 . **doi:** 10.1088/1674-1056/23/4/044501

A method for calibrating the confocal volume of a confocal three-dimensional micro-x-ray fluorescence setup*

Peng Zhou(周鹏)[1,2,3], Xin-Ran Ma(马欣然)[4], Shuang Zhang(张爽)[1,2,3], Tian-Xi Sun(孙天希)[1,2,3], and Zhi-Guo Liu(刘志国)[1,2,3,†]

[1] College of Nuclear Science and Technology, Beijing Normal University, Beijing 100875, China
[2] Applied Optics Beijing Key Laboratory, Department of Physics, Beijing Normal University, Beijing 100875, China
[3] Beijing Radiation Center, Beijing 100875, China
[4] Department of Physics, Beijing Normal University, Beijing 100875, China

(Received 28 October 2019; revised manuscript received 4 December 2019; accepted manuscript online 3 January 2020)

The measurement of the confocal volume of a confocal three-dimensional micro-x-ray fluorescence (3D-XRF) setup is a key step in the field of confocal 3D-XRF analysis. With the development of x-ray facilities and optical devices, 3D-XRF analysis with a micro confocal volume will create a great potential for 2D and 3D microstructural analysis and accurate quantitative analysis. However, the classic measurement method of scanning metal foils of a certain thickness leads to inaccuracy. A method for calibrating the confocal volume is proposed in this paper. The new method is based on the basic content of the textbook, and the theoretical results and the feasibility are given in detail for the 3D-XRF mono-chromatic x-ray condition and the poly-chromatic x-ray condition. We obtain a set of experimental confirmation using the poly-chromatic x-ray tube in the laboratory. It is proved that the sensitivity factor of the 3D-XRF can be directly and accurately obtained in a real calibration process.

Keywords: three-dimensional micro-x-ray fluorescence (3D-XRF), depth analysis, confocal volume, probe calibrating

PACS: 07.85.Tt, 07.85.Qe **DOI:** 10.1088/1674-1056/ab671c

1. Introduction

Three-dimensional micro-x-ray fluorescence (3D-XRF) has been an important analysis method in a large variety of fields[1][2,3] since Kanngießer *et al.* constructed the first 3D-XRF setup in 2003.[4] The depth resolution of 3D-XRF is determined by its confocal volume in full width at half maximum (FWHM), which also represents the best resolution for 2D or 3D mapping of the device. Therefore, the size of the confocal volume of each 3D-XRF needs to be accurately calibrated. The confocal volume of 3D-XRF is formed by the overlap of the output focal spot of the excitation channel and the input focal spot of the detection channel.[5] Usually, the depth resolution of a 3D-XRF setup as obtained by scanning metal foils of a certain thickness or wires using the classic method is given by[6]

$$D = (f^2 - d^2)^{1/2}, \tag{1}$$

where D is the depth resolution, which is the confocal volume in FWHM of the 3D-XRF setup; f is the FWHM of the intensity distribution curve when scanning the test metal foils or wires; and d is the thickness of the test foils or the diameter of the wires. In practice, the value of d that most researchers can obtain is generally 10–30 μm. The confocal volume size for FWHM in synchrotron radiation 3D-XRF has been reported to be ∼ 10–40 μm,[4,7–12] and that in desktop 3D-XRF has been reported to be ∼ 20–100 μm.[13–15]

The essence of this classic method is to convolve D using a convolution kernel with thickness d. Then the D can be calculated by the deconvolution method with the acquired experimental data. In the deconvolution process, the intensity of the confocal volume along the depth direction is usually expressed as a Gauss sensitivity function.[16] It can be demonstrated that the Gauss sensitivity function and its parameters can be obtained accurately with thin test foils.[16] However, the thin film (less than 1 μm) is difficult for most researchers to obtain and easily contaminated. Besides, the test process is too long due to the low counts of fluorescence.

In the present work, a new method is developed that accurately calibrates the size of the confocal volume. The detail theory and experimental process are presented in this work. A set of deconvolution result is obtained with this method. We compare this result with a common wire result in the discussion section. A brief outlook is given at the end of this work.

2. Theory

2.1. The sensitivity function of 3D-XRF

The sensitivity function characterizes the 3D-XRF setup from an experimental point of view. It was first proposed and

* Project supported by the National Natural Science Foundation of China (Grant Nos. 11675019 and 11875087).
† Corresponding author. E-mail: liuzhiguo512@126.com
© 2020 Chinese Physical Society and IOP Publishing Ltd

validated by Malzer and Kanngießer based on the textbook content. This sensitivity function consists of the transmission efficiency function of both excitation channel lens and the detection channel lens and the quantum efficiency of the corresponding detector, essentially depicting the spatial structure of the confocal volume. It should be pointed out that this function does not explicitly discuss the absorption effect of air and this part is included by default.[16]

In the work of 2005, by assuming the rotational symmetry, Malzer *et al.* used the two-dimensional Gaussian distribution function at both channel lenses to make a specific explanation, and obtained some results.[16] Experimentally, it should be pointed out that the sensitivity function is the quality function of the 3D-XRF system. In other words, the sensitivity function obtained from the experimental means is uniquely determined, and no matter which transmission efficiency distribution function of the lens is used to determine the size and shape of the confocal volume. We also cite this part of work in this paper, based on which we obtain the precise confocal volume.

2.2. Calibration model of the confocal volume in the case of mono-chromatic x-ray

First, in the case of a mono-chromatic excitation channel, there is a standard foil sample for scanning 3D-XRF. The thickness of this foil is very thin and the self-absorption effect can be neglected. Therefore, the fluorescence intensity ϕ is proportional to the mass deposition per area (Q in g/cm^2) of the foil. The intensity of a specific mono-chromatic x-ray in counts per second can be written as

$$\phi(z) = \phi_0 \eta(z) \sigma_F Q, \tag{2}$$

where ϕ_0 is the incoming flux in counts per second; $\eta(z)$ is the dimensionless sensitivity function along the Z axis[16] (refer to Fig. 1), where the FWHM of this distribution curve corresponds to the depth resolution; and σ_F is the production cross section (cm^2/g) for the corresponding x-ray line. Under this condition, the production cross section σ_F and the area density Q are constant coefficients. Therefore, the intensity distribution curve along the Z axis is positively correlated with the sensitivity distribution function $\eta(z)$. In other words, when the incoming flux ϕ_0 in counts per second is constant, the intensity distribution curve is completely coincident with the curve of the sensitivity distribution function $\eta(z)$. Therefore, it is easy to calculate the sensitivity distribution function $\eta(z)$. Usually, the function $\eta(z)$ can be assumed to have a Gaussian functional form, allowing a parameter σ_Z to be obtained for this sensitivity function, regardless of what the specific confocal volume looks like, where this parameter σ_Z is the standard deviation of the Gaussian function $\eta(z)$. So in Eq. (2), the parameters of the instrument sensitivity function $\eta(z)$ are the characteristic quantities for the 3D-XRF setup.[16]

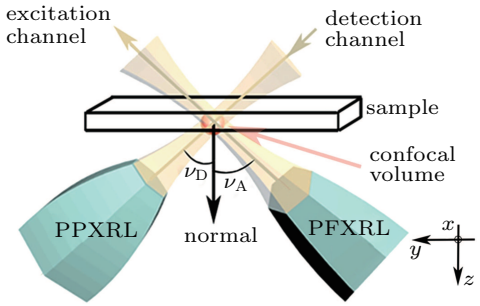


Fig. 1. Schematic diagram of the angles ν_A and ν_D.

Then, D can be calculated by

$$D = 2\sqrt{2\ln 2}\sigma_Z. \tag{3}$$

In this method, the required calibration samples are common and thick. For example, a 2.160 mm thick pure metal sample is used in this work. Such samples are easier to obtain for the researchers. The key point of this method is that the step size is set to the resolution of the controller (0.5 μm, or smaller) along the Z axis. When the calibration sample just convolutes the confocal volume along the Z-axis step by step, a set of data files (DF) can be obtained. This set of DF is named df_1, df_2, ..., df_n in turn. The theoretical number of counts of df_1 can be named $\phi(1)$. This condition can be written as

$$\phi(1) = \phi_0 \sigma_F \rho(\zeta) \eta_Z(z_{\zeta 1} - z_0), \tag{4}$$

where $\rho(\zeta)$ is the mass deposition per area under this condition, z_0 is the center of the confocal volume along the Z axis, $z_{\zeta 1}$ is the lower surface position of the calibration sample along Z axis (refer to Fig. 1), and $\eta_Z(z_{\zeta 1} - z_0)$ is the sensitivity value for this position in df_1. Usually, this sensitivity function can be written as

$$\eta_Z(z_{\zeta 1} - z_0) = \frac{\kappa}{\sqrt{2\pi}\sigma_Z} \exp\left(-\frac{(z_{\zeta 1} - z_0)^2}{2{\sigma_Z}^2}\right), \tag{5}$$

where σ_Z is the standard deviation of the sensitivity function of the 3D-XRF setup along the Z axis and κ is a constant related to the polycapillary lens transmission efficiency and detector efficiency.

Then, the theoretical number of counts of df_2, $\phi(2)$, can be written as

$$\begin{aligned}\phi(2) = {} & \phi_0 \sigma_F \rho(\zeta) \eta_Z(z_{\zeta 2} - z_0) \\ & + \phi(1) \exp\left(-\left(\frac{u_{e,j}}{\cos \nu_A} + \frac{u_{f,j}}{\cos \nu_D}\right) d\right),\end{aligned} \tag{6}$$

where $\eta_Z(z_{\zeta 2} - z_0)$ is the sensitivity value for the current lower surface position of the calibration sample, $u_{e,j}$ is the mass attenuation coefficient (cm^2/g) for the energy of excitation in element j, $u_{f,j}$ is the mass attenuation coefficient for the detected line, d is the step size, and ν_A and ν_D are the

related angles shown in Fig. 1. In this section, we only discuss the case of monochromatic condition, the polychromatic condition is discussed in the following sections.

Therefore, as the calibration sample is shifted step by step, the theoretical number of counts of df_i, $\phi(i)$, can be written as

$$\phi(i) = \phi_0 \sigma_{\mathrm{F}} \rho(\zeta) \eta_Z(z_{\zeta i} - z_0) + \phi(i-1) \exp\left(-\left(\frac{u_{\mathrm{e},j}}{\cos \nu_{\mathrm{A}}} + \frac{u_{\mathrm{f},j}}{\cos \nu_{\mathrm{D}}}\right) d\right), \quad (7)$$

where $z_{\zeta i}$ is the current lower surface position of the sample, $\eta_Z(z_{\zeta i} - z_0)$ is the sensitivity value for this current lower surface position, and $\phi(i-1)$ is the theoretical number of counts of df_{i-1}.

This model can be simulated with a computer program to find the best parameters via

$$\mathrm{sum}(C, z_0, \sigma_Z) = \sum_{i=1}^{n} [\phi(i) - \mathrm{Data}(i)]^2, \quad (8)$$

where the sum function is the target function simulated to obtain the minimum value; C is a constant, representing the value of $\phi_0 \sigma_{\mathrm{F}} \rho(\zeta) \kappa$; z_0 is the target center of the confocal volume of the 3D-XRF setup along the Z axis; σ_Z is the standard deviation, corresponding to the FWHM in Eq. (3); n is the total number of DF; $\phi(i)$ denotes the simulated theoretical data; and $\mathrm{Data}(i)$ denotes the real experimental data corresponding df_i. The minimum $\mathrm{sum}(C, z_0, \sigma)$ can be found by varying the parameters C, z_0, and σ_Z in the simulations.

2.3. Calibration model of the confocal volume in the case of poly-chromatic x-ray

Poly-chromatic x-ray occurs mostly in the laboratory 3D-XRF, usually the target of the x-ray sources is molybdenum. When the calibration sample convolutes the confocal volume along the Z-axis step by step, a set of DF in this polychromatic condition can also be obtained. This set of DF is also named df_1, df_2, ..., df_n in turn. The theoretical number of counts of df_1 can be named $\phi(1)$. This $\phi(1)$ can be written as

$$\phi(1) = \int_{E_{\mathrm{abs}}}^{E_{\max}} \phi(1, E) \mathrm{d}E, \quad (9)$$

where E_{abs} is the absorption limit of the sample and $E_{\max}$ is the upper limit of the spectral energy. $\phi(1, E)$ is the fluorescence count produced by a particular energy line. All the counts of $\phi(1)$ are counted from these energy ranges. $\phi(1, E)$ can be written as

$$\phi(1, E) = \phi_0 I_0(E) \sigma_{\mathrm{F},E} \rho(\zeta) \eta_{Z,E}(z_{\zeta 1} - z_0), \quad (10)$$

where $I_0(E)$ is the normalized intensity distribution of the spectrum, and the sensitivity function can be re-written as

$$\eta_{Z,E}(z_{\zeta 1} - z_0) = \frac{\kappa_E}{\sqrt{2\pi}\sigma_{Z,E}} \exp\left(-\frac{(z_{\zeta 1} - z_0)^2}{2{\sigma_{Z,E}}^2}\right), \quad (11)$$

where $\sigma_{Z,E}$ is the standard deviation of the sensitivity function in the specific x-ray line of the 3D-XRF setup along the Z axis and κ_E is a constant related to the polycapillary lens transmission efficiency in the specific x-ray energy and detector efficiency. Here, κ_E is not expanded according to the excitation end and the detection end. Then, the theoretical number of counts of df_2, $\phi(2)$, can be written as

$$\phi(2) = \int_{E_{\mathrm{abs}}}^{E_{\max}} \phi_0 I_0(E) \sigma_{\mathrm{F},E} \rho(\zeta) \eta_{Z,E}(z_{\zeta 2} - z_0) \mathrm{d}E + \phi(1) \exp\left(-\left(\frac{u_{E,j}}{\cos \nu_{\mathrm{A}}} + \frac{u_{\mathrm{f},j}}{\cos \nu_{\mathrm{D}}}\right) d\right), \quad (12)$$

where $u_{E,j}$ is the mass absorption coefficient of the different energy x-rays (E) in the sample element j. The value of d in this work is set to 5×10^{-4} cm, so $u_{E,j}$ in Eq. (12) has little contribution to $\phi(2)$. Therefore, we can write it as $u_{\mathrm{e},j}$. Theoretically, the d slightly changes with $I_0(E)$ according to the energy. As the total intensity ϕ_0 is properly attenuated, due to this effect, it is not significant, we can use $u_{\mathrm{e},j}$ to simplify the model. Therefore, as the calibration sample is shifted step by step, the theoretical number of counts of df_i, $\phi(i)$, can be written as

$$\phi(i) = \int_{E_{\mathrm{abs}}}^{E_{\max}} \phi_0 I_0(E) \sigma_{\mathrm{F},E} \rho(\zeta) \eta_{Z,E}(z_{\zeta i} - z_0) \mathrm{d}E + \phi(i-1) \exp\left(-\left(\frac{u_{\mathrm{e},j}}{\cos \nu_{\mathrm{A}}} + \frac{u_{\mathrm{f},j}}{\cos \nu_{\mathrm{D}}}\right) d\right), \quad (13)$$

where $z_{\zeta i}$ is the current lower surface position of the sample, $\eta_{Z,E}(z_{\zeta i} - z_0)$ is the sensitivity value for this current lower surface position, and $\phi(i-1)$ is the theoretical number of counts of df_{i-1}.

Here, we have to figure out $I_0(E)$, $\sigma_{\mathrm{F},E}$, $\sigma_{Z,E}$, and κ_E. Only in this way can we accurately discuss Eq. (13). For the x-ray primary spectrum, the researchers proved that it can be calculated.[17] Many researchers have calculated and experimentally determined the intensity distribution of the primary x-ray spectrum.[18–24] The continuum can be described by some expressions,[19,23] and the ratio of the characteristic spectrum and the continuum at a specific wavelength can be accurately calculated.[19] So $I_0(E)$ is a mathematically very clear cross-sectional distribution. Tao *et al.*[25] used NRLXRF,[18] NBS,[19] and Planitz–Penno[22] to calculate the relative intensity of a series of primary x-ray lines and to quantitatively analyze some elements, such as calcium (Ca), iron (Fe), nickel (Ni), zinc (Zn), and lead (Pb). The analysis showed that the quantitative fluorescence results calculated by different programs were slightly different, but the relative deviation did not exceed 1%.[25] Therefore, primary x-ray spectroscopy morphologies can be described by functional expressions and have no significant effect on the polychromatic integral fluorescence quantification of different identified elements. In addition, Green *et al.*[26–28] demonstrated that for

pure light element targets (such as molybdenum, copper, etc.), the K-series characteristic x-rays are mainly generated by direct electron impact and the output efficiency can be theoretically determined, and the continuum can be studied from a similar approach. The work of Green *et al.* is consistent with the experimental results well.

The confocal volume is determined by the sizes of the focal spots of the excitation and detection channel lenses. For polychromatic excitation, Mantouvalou *et al.*[29] used different tube voltages for calibration with different identified elements (i.e., Cr, Fe, Cu, Zn, and Pb). Based on the premises that the transmission efficiency section of the excitation channel lens is determined and that the primary x-ray spectrum is calculated, the results show that increasing the tube voltage causes the whole spectrum to shift toward high energies and the size of the excitation lens's focal spot to decrease; however, the change is not significant because the experimentally calibrated confocal volume does not change significantly.[29] In fact, the size of the actual confocal volume in the case of poly-chromatic x-ray excitation depends mainly on the characteristic energy of the sample element, and has little relationship with the actual incident x-ray intensity distribution. This is because when the confocal volume is calibrated for the characteristic energy corresponding to different elements, the state of the incident end is always the same, regardless of the incident spectral distribution of the device and the transmission efficiency of the lens. The size of the final calibrated volume depends on the characteristic energy and the lens quality at the detector end. The same is true for the process of actually testing an unknown sample, so the size of the volume calibrated in this way is more accurate and conforms to the actual engineering conditions. Therefore, the κ_E can be replaced with κ, the $\sigma_{Z,E}$ can be replaced by the effective factor $\sigma_{Z,\mathrm{eff}}$. The $\sigma_{\mathrm{F},E}$ can be extracted from the fundamental parameter databases,[30] typically for a particular excited sample element, it is a constant σ_{F}. In summary, it can be see from Eq. (13) that the calculation method of $\phi(i)$ for the poly-chromatic x-ray condition is analogous to that for the mono-chromatic x-ray condition. So a monochromatic 3D-XRF spectrometer can obtain results using the basic parameter method, whereas a polychromatic 3D-XRF spectrometer can achieve the same results by extending the basic parameters to effective parameters.

It is worth noting that the lens attached in the detection channel has difference sizes of the confocal volume for different energies.[31] Therefore, the confocal volume needs to be experimentally calibrated for each identified element. Then, this model can be simulated with a computer program to find the best parameters via

$$\mathrm{sum}\,(C, z_0, \sigma_{Z,\mathrm{eff}}) = \sum_{i=1}^{n} [\phi(i) - \mathrm{Data}\,(i)]^2, \qquad (14)$$

where the sum function is the target function simulated to obtain the minimum value; C is a constant, representing the value of $\phi_0 \sigma_{\mathrm{F}} \rho\,(\zeta)\,\kappa$; z_0 is the target center of the confocal volume of the 3D-XRF setup along the Z axis; $\sigma_{Z,\mathrm{eff}}$ is the standard deviation, corresponding to the FWHM in Eq. (3); n is the total number of DF; $\phi(i)$ denotes the simulated theoretical data; and $\mathrm{Data}\,(i)$ denotes the real experimental data corresponding to df_i. The minimum $\mathrm{sum}\,(C, z_0, \sigma_{Z,\mathrm{eff}})$ can also be found by varying the parameters C, z_0, and $\sigma_{Z,\mathrm{eff}}$ in the simulations.

3. Experiment and discussion

3.1. Confocal 3D-XRF setup

Figure 1 shows a schematic diagram of the confocal geometry, where the confocal volume is the overlap of the output focal spot of the polycapillary focusing x-ray lens (PFXRL)[5] and the input focal spot of the polycapillary parallel x-ray lens (PPXRL).[5] An x-ray source with a Mo target (XTG Ultra-Bright Micro-focus X-ray Source, Oxford, USA) was used.[5] The PFXRL for x-ray irradiation was attached to the x-ray source, and the PPXRL was attached to a silicon drift detector (Si-PIN) (X-123, Amptek, USA), (sensitive area: 6 mm^2, energy resolution: 145 eV at 5.9 keV). Each polycapillary lens was designed and manufactured by the College of Nuclear Science and Technology, Beijing Normal University.[5] The input focal distance of the PFXRL was 52.9 mm, and the output focal distance of the PFXRL was 11.5 mm. The focal distance of the PPXRL was 14.9 mm. The focal spot size of the PFXRL was experimentally evaluated to be 32.4 μm at 17.4 keV (Mo $K\alpha$); and that of PPXRL was 33.0 μm under the same condition. Both polycapillary x-ray lenses were positioned in the confocal geometry. The angle between the incident and detection beams was set to 90°.[5] The sample stage was installed on an X–Y–Z stage (DS102 Series, SURUGA SEIKI, Japan) with a step resolution of 0.5 μm on each axis. A CCD camera was also used to watch the relative position between the sample and the marked position of the confocal volume.[5]

3.2. Experiments and discussion

In order to verify the method, in this work, the method for calibrating the depth resolution of the setup at the energy of Ni $K\alpha$ was operated by testing a standard nickel sample. The x-ray source was operated at 20 kV and 0.5 mA. The pure nickel sample was placed on the sample stage and tested in the positive direction of the Z axis (refer to Fig. 1). The sample stage moved step by step with the minimum resolution of the controller, and the test time per step was 60 s. Then we imported this set of data DF into our own program for simulation, the program is written in MATLAB. In the preprocessing of the DF, in order to eliminate the influence of fluctuations and other factors, we smoothed the actual DF (refer to the data curve in Fig. 2) by multi-points smooth method and renewed

the DF (refer to the smooth data curve in Fig. 2). The minimum sum $(C, z_0, \sigma_{Z,\text{eff}})$ was found by simulating the renewed DF. The value of C was found to be 158706 counts/s, z_0 was found to correspond to the 212nd of the 504 points of the experimental data DF, and the value of $\sigma_{Z,\text{eff}}$ was found to be 28.0913 μm, meaning that the FWHM of the simulated curve along the Z axis was 66.15 μm. Figure 2 compares the experimental distribution curve and the simulated distribution curve obtained with MATLAB. Essentially, the experimental curve is the f in Eq. (1), and the simulated curve is the D of Eq. (1). As seen from Fig. 2, the simulated curve fits the experimental data curve well. This illustrates that the theoretical model is correct and the convolution kernel d can be very small in a practical calibration process.

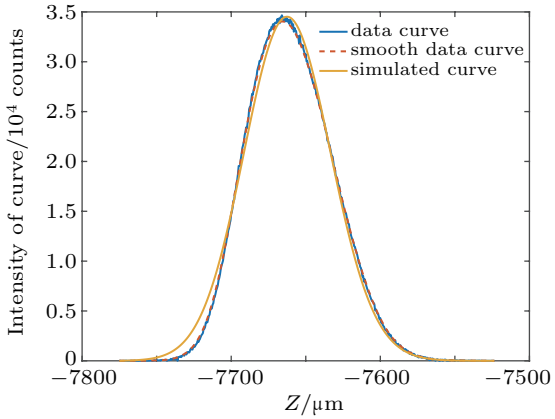


Fig. 2. MATLAB-fitted curve from the simulation.

In fact, the method provides a deconvolution layer to obtain the intensity distribution of the confocal volume. It can provide a good analytical depth resolution if we test samples along Z axis as shown in Fig. 1. This is because the quantity fluorescence counting is related to a local layer density function in the common fundamental parameters model and this kind of layer is perpendicular to the Z axis.[32] We found that the depth resolution was 75 μm at the energy of Ni $K\alpha$ using a 20 μm nickel wire.[5] It indicates that the wire can not obtain a depth resolution result using the layer model in deconvolution process. Besides, the convolution kernel width and the geometric shape of the wire will lead to inaccuracy in the calibration process. Therefore, the new method proposed in this paper can be a better choice to use in a real calibration process.

It should be pointed out that the simulated peak position is slightly shifted to the right by less than 3.5 μm. This is because the confocal volume composed of the actual hexagonal lenses is not a Gaussian distribution in the strict sense, so the resulting fit is not strictly consistent. Besides, this movement is not significant and does not affect the size of the actual calibrated volume. Overall, the experimental results are a good proof of the correctness of the calibration model. Detailed mathematical models have been presented in Section 2. This method suits for obtaining the confocal volume at different x-ray energies, such as Zn $K\alpha$ and Pb $L\alpha$ according to requirement. We hope that this more accurate calibration model can be widely used as an alternative measurement scheme because accurately calibrating the probe size is an important part of fluorescence analysis. Besides, this new method provides ideas and feasibility for deconvolution of the confocal volume in three dimensions.

In the future research work, we will give a more specific transmission efficiency distribution function according to the geometry and characteristics of the capillary lens used on the 3D-XRF, especially in the case of a regular hexagonal polycapillary lens. This approach is critical to the precise quantitative analysis process if the characteristics of volume can be accurately measured.[29,32] One the other hand, we think that metaheuristic algorithms[33–37] (differential evolution, particle swarm optimization, etc.) can be used for solving Eq. (14). We hope to report good results in the future.

4. Conclusion

A method for accurately obtaining the confocal volume of a confocal 3D-XRF setup is demonstrated. The size of the confocal volume can be accurately measured at different x-ray energies with this method. Therefore, this method provides better support for accurate 2D or 3D analysis of samples with fine microstructures and for quantitative analysis.

The disadvantage of the method is that the x-ray spot is not uniform. It should be confirmed whether the polycapillary lens attached at the excitation channel is in the best position relative to the x-ray tube. Additionally, a theoretical model of the experimental absorption enhancement effect will require further development using advance Monto Carlo algorithm or more accurately reproduce experimental measurements with multi-elements samples.

Acknowledgment

Thanks to Yuelin Zhang for the testing sample.

References

[1] Yi L T, Liu Z G, Wang K, Lin X, Chen M, Peng S, Yang K and Wang J B 2016 *Appl. Phys. A* **122** 329
[2] Bruyndonckx P, Sasov A and Liu X 2010 *AIP Conf. Proc.* **1365** 61
[3] Peng S, Liu Z G, Sun T X, Ma Y and Ding X L 2014 *Anal. Chem.* **86** 362
[4] Kanngießer B, Malzer W and Reiche I 2003 *Nucl. Instrum. Methods Phys. Res. Sect. B Beam Interact. Mater. Atoms* **211** 259
[5] Zhou P, Liu Z G, Lin X Y, Liu X, Ye L, Wang X Y, Pan K and Li Y D 2018 *Nucl. Instrum. Methods Phys. Res. Sect. B Beam Interact. Mater. Atoms* **423** 37
[6] Gao N and Janssens K 2004 *Polycapillary x-ray optics* (Chichester: John Wiley & Sons, Ltd) p. 89
[7] Janssens K, Proost K and Falkenberg G 2004 *Spectrochim. Acta - Part. B At. Spectrosc.* **59** 1637

[8] Wilke M, Appel K, Vincze L, Schmidt C, Borchert M and Pascarelli S 2010 *J. Synchrotron Radiat.* **17** 669

[9] Kanngießer B, Mantouvalou I, Malzer W, Wolff T and Hahn O 2008 *J. Anal. At. Spectrom.* **23** 814

[10] Woll A R, Mass J, Bisulca C, Huang R, Bilderback D H, Gruner S and Gao N 2006 *Appl. Phys. A* **83** 235

[11] De Samber B, Silversmit G, De Schamphelaere K, Evens R, Schoonjans T, Vekemans B, Janssen C, Masschaele B, Van Hoorebeke L, Szalóki I, Vanhaecke F, Rickers K, Falkenberg G and Vincze L 2010 *J. Anal. At. Spectrom.* **25** 544

[12] Vincze L, Vekemans B, Brenker F E, Falkenberg G, Rickers K, Somogyi A, Kersten M and Adams F 2004 *Anal. Chem.* **76** 6786

[13] Smolek S, Pemmer B, Fölser M, Streli C and Wobrauschek P 2012 *Rev. Sci. Instrum.* **83** 083703

[14] Sun T X, Liu Z G, Li Y D, Lin X Y, Wang G, Zhu G, Xu Q, Luo P, Pan Q L, Liu H and Ding X L 2010 *Nucl. Instrum. Methods Phys. Res. Sect. A Accel. Spectrometers Detect. Assoc. Equip.* **622** 295

[15] Kanngießer B, Malzer W, Rodriguez A F and Reiche I 2005 *Acta - Part. B At. Spectrosc.* **60** 41

[16] Malzer W and Kanngieer B 2005 *Spectrochim. Acta - Part. B At. Spectrosc.* **60** 1334

[17] Ebel H 1999 *X-Ray Spectrom.* **28** 255

[18] Griss J W 1997 *NRLXRF, COSMIC Program and Documentation DOD-65*, Computer software management and information center, University of Georgia, USA

[19] Pella P A, Feng L and Small J A 1985 A *X-Ray Spectrom.* **14** 125

[20] Gilfrich J V and Birks L S 1968 *Anal. Chem.* **40** 1077

[21] Brown D B, Gilfrich J V and Peckerar M C 1975 *J. Appl. Phys.* **46** 4537

[22] Planitz-Penno S, Schytte U, Stork G and Fresenius Z 1982 *Anal. Chem.* **312** 600

[23] Pella P A, Feng L and Small J A 1991 *X-Ray Spectrom.* **20** 109

[24] Murata M and Shibahara H 1981 *X-Ray Spectrom.* **10** 41

[25] Tao G Y and Zhuo S J 1998 *Acta Chim. Sin.* **56** 873 (in Chinese)

[26] Green M and Cosslett V E 1968 *J. Phys. D:Appl. Phys.* **1** 425

[27] Green M, Cosslett V E, Archard G D and Mulvey T 1964 *Proc. Phys. Soc.* **83** 435

[28] Pavlinsky G V and Lavrent Y G 1961 *Proc. Phy. Soc.* **78** 1206

[29] Mantouvalou I, Wolff T, Seim C, Stoytschew V, Malzer W and Kanngießer B 2014 *Anal. Chem.* **86** 9774

[30] Elam W T, Ravel B D and Sieber J R 2002 *Radiat. Phys. Chem.* **63** 121

[31] Wolff T, Mantouvalou I, Malzer W, Nissen J, Berger D, Zizak I, Sokaras D, Karydas A, Grlj N, Pelicon P, Schütz R, Žitnik M and Kanngießer B 2009 *J. Anal. At. Spectrom.* **24** 669

[32] Mantouvalou I, Malzer W and Kanngießer B 2012 *Spectrochim. Acta - Part. B At. Spectrosc.* **77** 9

[33] Zhou P, Ma X R, Zhang S, Liu Z G, Meng Z Y, Xiang Z J, Wang X Y, Sun T X, Lin X Y and Li Y D 2019 *Nucl. Instrum. Methods Phys. Res. Sect. A Accel. Spectrometers Detect. Assoc. Equip.* **953** 163077

[34] Gao P Y, Lv J, Wang Y C and Ma Y M 2017 *Physics* **46** 582 (in Chinese)

[35] Zhou P, Ma Y X, Wang X L, Ma H T, Xu X J and Liu Z J 2010 *High Laser Part. Beams.* **22** 973

[36] Civicioglu P and Besdok E 2013 *Artif. Intell. Rev.* **39** 315

[37] Wang K, Liu G, Li Y C, Wang J B and Wang G 2019 *Powder Technol.* **344** 598